Inter–pixel grating noise in holographic memories

Xin An, George Panotopoulos, and Demetri Psaltis

Department of Electrical Engineering,
California Institute of Technology, Mail Stop 136-93,
Pasadena, CA 91125
e-mail: axin,gpano,psaltis@sunoptics.caltech.edu

ABSTRACT

We have experimentally discovered that the Signal–to–Noise Ratio (SNR) of holograms initially remains constant as the number of holograms stored increases and drops significantly only after a large number of holograms are recorded. This suggests that in a large–scale memory, the limiting noise source is not crosstalk between holograms but holographic noise due to the prolonged exposure of the signal beam. We have carried out experiments to investigate the formation and influence of the inter–pixel grating noise and shown that it is a very important form of holographic noise. We also proposed and demonstrated the use of random–phase modulation in the signal to suppress the inter–pixel grating noise.

Keywords: holographic memory, $LiNbO_3$:Fe, inter–pixel grating noise, random–phase modulation

1. INTRODUCTION

Inter–pixel grating noise is a very important yet largely ignored form of holographic noise. It is a secondary effect—the secondary diffraction (rediffraction) of the diffracted signal upon reconstruction, via the gratings formed between the multiple plane–wave (spatial–frequency) components of the signal. In Fourier–transform–plane recording, the inter–pixel grating noise can be considered as crosstalk noise between the pixels within a page of data, similar to a class of higher–order crosstalk noise in volume holographic interconnections.[1] During holographic recording, the plane waves originated from the pixels on the Spatial Light Modulator (SLM) interfere with the reference beam to form the "useful" information hologram. In the meantime, they interfere with each other to create noise gratings. Upon readout, the same reference beam is used to reconstruct the plane waves, which are converted back to the corresponding pixels by imaging optics for data retrieval. In addition, these reconstructed plane waves give rise to secondary diffraction (rediffraction) via the noise gratings, resulting in crosstalk among the pixels. This is the reason that we name this noise source inter–pixel grating noise*.

Figure 1 shows a simple example of the inter–pixel grating noise. $\vec{K}_i$ and $\vec{K}_j$ are the wave–vectors of two plane waves corresponding to two pixels i, j in the image. $\vec{K}_r$ is the reference beam wave–vector. The gratings $\vec{K}_{ri}$ and $\vec{K}_{rj}$ are the "useful" ones, responsible for information storage and retrieval. Upon readout, the "output" pixel j receives light from the reference via grating $\vec{K}_{rj}$. In addition, it receives light from pixel i through the intermediate step of diffraction by grating $\vec{K}_{ri}$ followed by rediffraction via grating $\vec{K}_{ij}$. This additional light is the inter–pixel grating noise.

It should be noted that the inter–pixel gratings noise exists, though in different forms, when other recording configuration such as Fresnel–plane or image–plane recording is used. In such occasions, it arises from the crosstalk between the spatial–frequency components of the signal†.

Inter–pixel gratings are often assumed to be very weak because of two reasons: their large grating periods and small modulation depths. The first is the result of the small angles between the plane–wave components. The second one is due to the simple fact that the power a pixel carries is orders of magnitudes less than that of the reference beam. However, in a large–scale holographic memory using $LiNbO_3$:Fe crystals, the inter–pixel grating noise is indeed a very important noise source because of

*A similar term—"inter–pixel noise" is used to indicate the crosstalk among the pixels due to their finite sizes and limited optical aperture of the system.[2,3]

†Therefore, a better name might be "intra–hologram crosstalk", as opposed to the "inter–hologram crosstalk".

Part of the SPIE Conference on Advanced Optical Memories and Interfaces to Computer Storage • San Diego, California • July 1998
SPIE Vol. 3468 • 0277-786X/98/$10.00

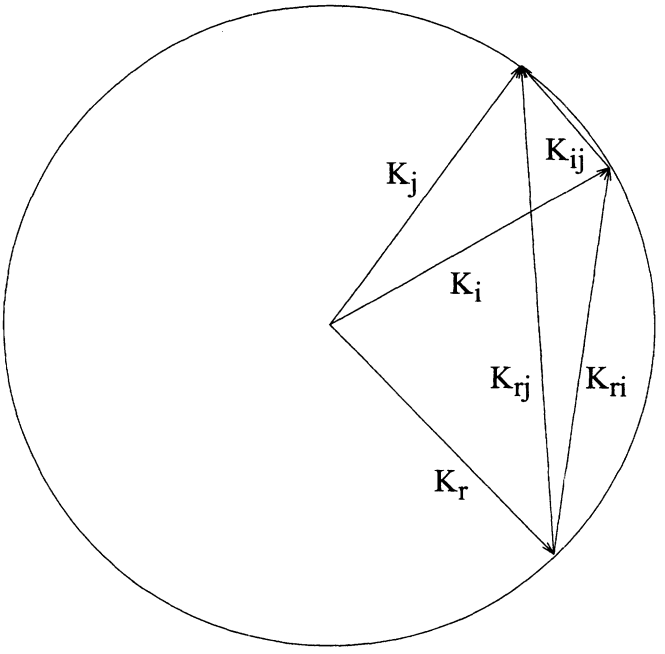

Figure 1. K–space description of inter–pixel grating noise.

- the presence of strong photovoltaic effect in photovoltaic materials such as $LiNbO_3$:Fe, which overwhelms diffusion as the dominant charge transport mechanism and enables effective holographic recording of gratings even with very large periods;
- the prolonged and repeated exposure for multiple–hologram recording which allows the inter–pixel gratings to be strengthened many times;
- the collective behavior of a large number of pixels made possible by higher degree of Bragg degeneracy and weak Bragg selectivity among the pixels.

The influence of the inter–pixel grating noise should become stronger as the total exposure or the total number of holograms stored increases. In addition, one must note that the inter–pixel grating noise is a global effect—any hologram shall see the same level of noise regardless of its temporal position in the recording sequence and its physical address in the memory. However, the amount of noise that an individual pixel sees also depends on its spatial location in the image and the its neighborhood.

2. CHARACTERIZATION OF SYSTEM ERROR PERFORMANCE

We conducted a series of experiments to evaluate the system error performance and characterize the effect of the inter–pixel grating noise using the Signal–to–Noise Ratio (SNR) as the system metric. The experimental setup is shown in Figure 2. It is capable of storing up to 160,000 holograms using angle, fractal, and spatial multiplexing.[4] The storage material, a 90°–geometry $LiNbO_3$:Fe crystal was placed on the Fourier–transform plane. A random–phase diffusor was used to spread out the DC intensity in the Fourier spectrum. We analyzed the SNR of the reconstructions from a single, 100, 300, 1,000, 5,000, and 10,000 holograms stored in the same volume by angle and fractal multiplexing. All the holograms were recorded to the same strength using the same exposure schedule[5] with the same last exposure time. To avoid significant noise buildup due to long exposures at the beginning, we did not use the full dynamic range of the storage system. The inter–hologram spacing was set at four times wider than the measured Bragg selectivity to reduce the ("inter–hologram") crosstalk noise.

The measured SNR as a function of the number of holograms stored is plotted in Figure 3. It shows that the SNR initially remains nearly constant as the number of holograms stored increases and drops only after a large number of holograms are recorded. This suggests that "inter–hologram" crosstalk noise is very unlikely to be responsible for

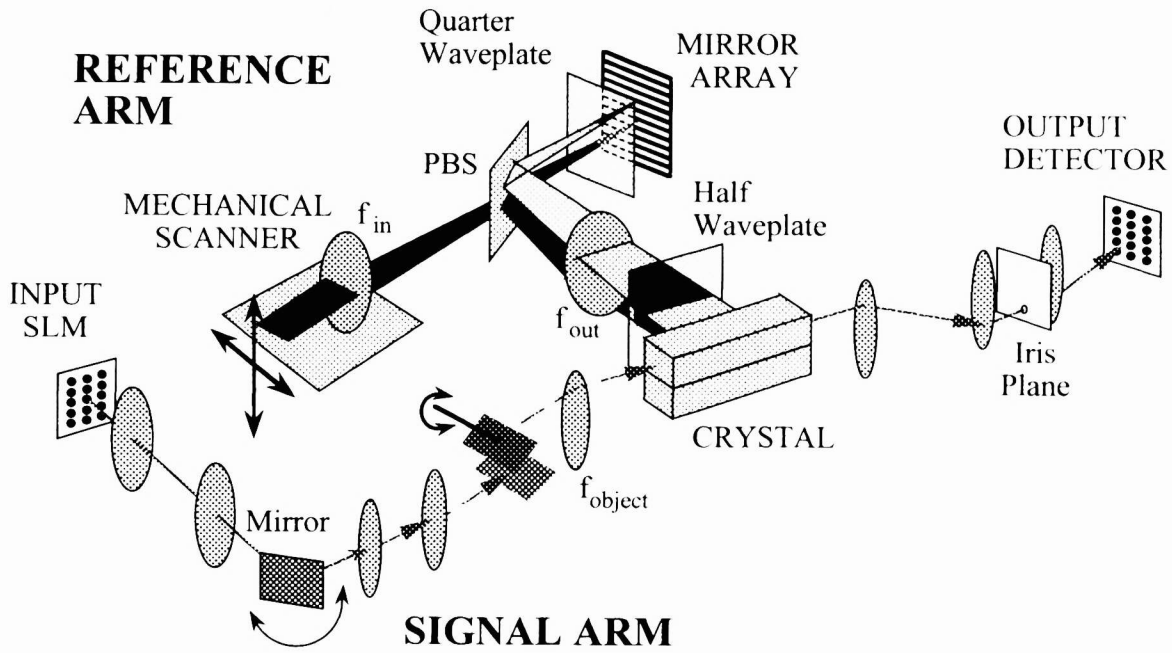

Figure 2. Experimental setup of the large-scale memory.

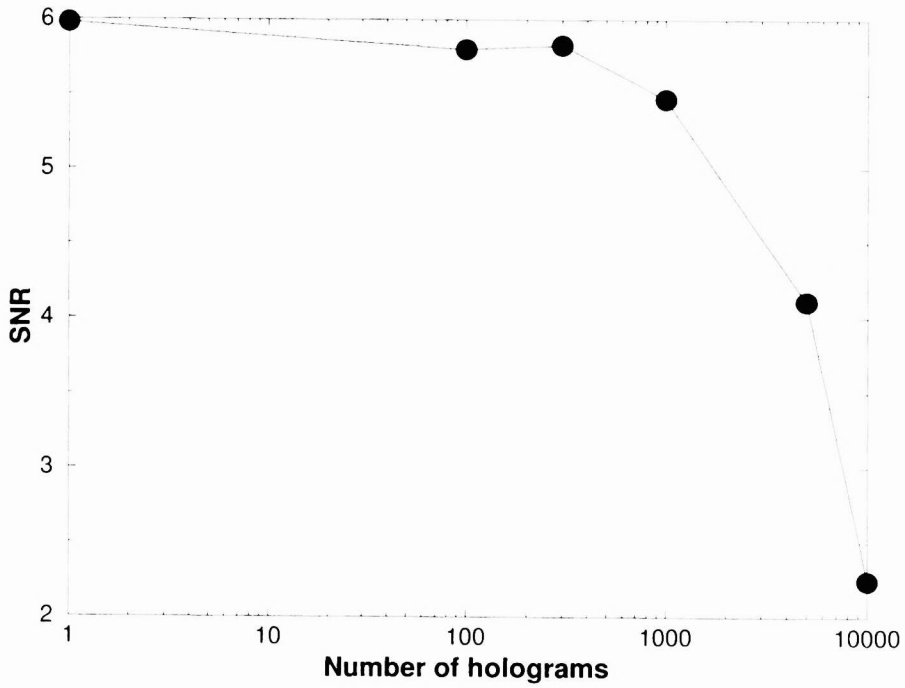

Figure 3. SNR degradation as a function of the number of holograms.

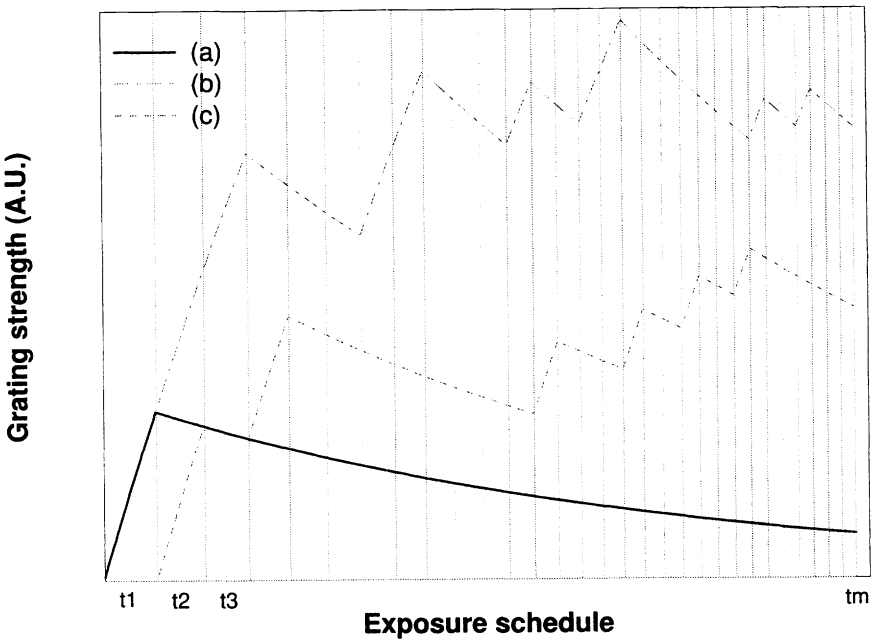

Figure 4. Different recording and erasure behaviors of (a) an information grating and (b)(c) inter–pixel gratings during multiple hologram recording.

the degradation of system error performance since its effect is local. The crosstalk noise shall initially build up as the number of holograms becomes larger and reach a "plateau" when holograms further recorded are too far away to contribute noticeable noise[‡]. The significant drop in the SNR as the number of holograms becomes larger indicates that the dominant noise source depends strongly on the total exposure. Noise sources that depend on the exposure during holographic recording are always associated with the buildup of noise gratings between various sources—the writing beams, their scattering off the holographic gratings and the impurity centers inside the material. Among them, there are two–beam coupling, fanning, and inter–pixel grating noise. Two–beam coupling can be neglected becasue it requires very strong holograms to cause the interaction between the writing beams. Fanning noise, which can be treated as the enhanced scattering, tends to cluster along the writing beams. It is greatly reduced by 90°–geometry recording. Inter–pixel grating noise, on the other hand, always exists and grows significantly during multiple–hologram recording.

3. BUILDUP OF INTER–PIXEL GRATINGS

For multiple hologram recording in $LiNbO_3$, an exposure schedule is used to equalize the strength of all the holograms. Each "useful" (information) grating in a hologram (e.g., $\vec{K}_{rj}$ in Figure 1) is recorded for a certain amount of time according to the exposure schedule, and then erased during the recording of the rest of the holograms with different reference $\vec{K}_r$'s. This is shown in Figure 4(a). To the contrary, an inter–pixel grating formed by two plane–wave components (e.g., $\vec{K}_{ij}$ in Figure 1) is recorded for many times, whenever both pixels i, j are ON at the same time. If we assume that the images to be stored in the memory are uncorrelated pages of binary data, the possibilities of a pixel to be either ON or OFF are the same across the entire image and from image to image. Therefore, during holographic recording of M holograms, one inter–pixel grating is strengthened repeatedly, for $M/4$ times on average (Figure 4(b)(c)). As a result, the final diffraction efficiencies of the inter–pixel gratings strongly depend on the total number of holograms and can be conceivably large compared to that of one information grating.

To investigate the buildup of inter–pixel gratings, we carried out another series of experiments using the same setup. In the signal arm, the SLM and following imaging and Fourier–transform optics were removed. Instead, we

[‡]The drop in the SNR of reconstructions from a few hundred holograms should be closely related to the ("inter–hologram") crosstalk.

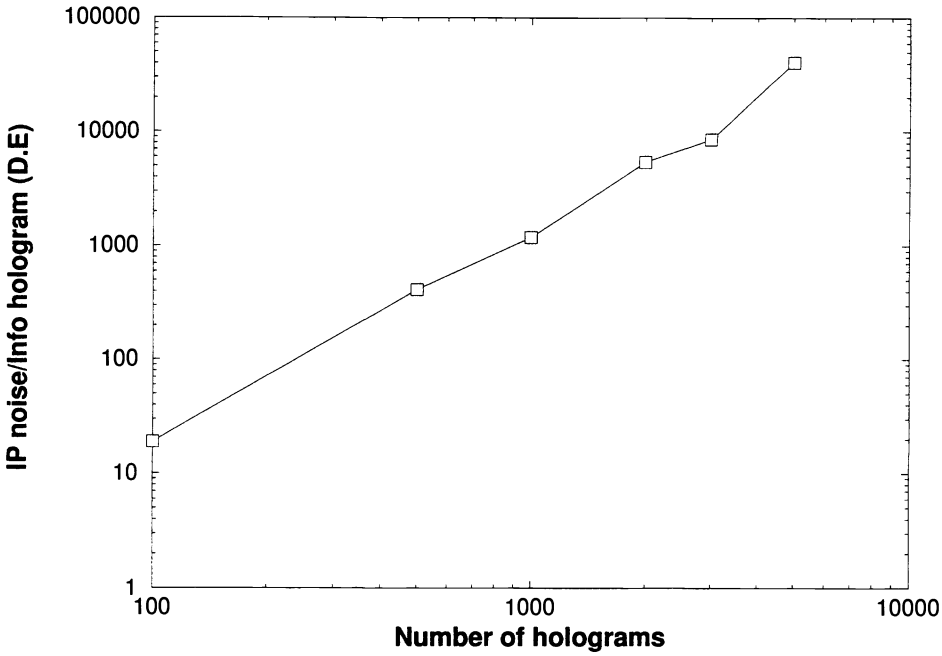

Figure 5. Ratio of the diffraction efficiencies of the inter–pixel grating and the information hologram as a function of the number of holograms.

used two plane waves to represent two pixels at the Fourier plane. The two plane waves were set apart horizontally by an outside angle of 1°. Two shutters were used to control the ON/OFF states of the two beams independently to form a random 2–bit signal. The crystal was exposed by a sequence of random 2–bit patterns according to an exposure schedule. Ideally, since the inter–pixel gratings are written by the plane-wave components in the complex signal, to reveal their evolution in multiple–hologram recording, we can simply illuminate the crystal with the signal beam with the exposure schedule. This procedure is much easier because holographic recording is not involved. It is also free of the noise caused by illumination of the reference beam . However, because we did not have a large number of plane waves (pixels), the ON/OFF states of the two beams significantly affected the total light intensity, thus the buildup rate of the inter–pixel grating. Therefore, a strong reference beam was used to actually record holograms using the exposure schedule. The intensity ratio of the reference beam and each of the plane–wave signal was set at more than 10. This guaranteed that the total exposing light intensity, hence the time constant, remained nearly the same regardless of the ON/OFF states of the two signal beams. We stored 10, 100, 300, 1,000, 2,000, 3,000, and 5,000 random 2–bit holograms. The same exposure schedule with the same last exposure time was used to record equalized holograms with the same strength. At the end of the recording, one of the signal beams was turned on and its diffraction into the other one via the inter–pixel grating was monitored by a photodetector. The readout was used to calculate the diffraction efficiency of the inter–pixel grating and compared to that of the information hologram reconstructed by the reference beam. Figure 5 summaries the results where the ratio of the diffraction efficiencies of the inter–pixel grating and the information hologram is plotted as a function of the number of holograms stored.

As shown in Figure 5, the inter–pixel grating increases significantly by repeated strengthening as the number of holograms stored becomes larger. After 5,000 holograms are stored, the inter–pixel grating is about 4×10^4 times stronger than the (information) hologram! However, we must note that, the modulation depth of this inter–pixel grating is much larger than that in a practical case where a large amount of pixels are involved. In order to predict the growth of the inter–pixel gratings in a real case, we numerically simulated holographic recording based on the Kukhtarev equations.[6] In the analysis, the set of partial, non–linear differential equations were simplified to form two linear differential equations governing the evolution of the DC and 1^{st}–order components of the space–charge field.[7] The 4^{th}–order Rouge–Kutta method was used to evaluate these two equations using a set of parameters similar to the ones found in previous works.[8] An inter–pixel grating $\vec{K}_{ij}$ was assumed to be formed between a pair

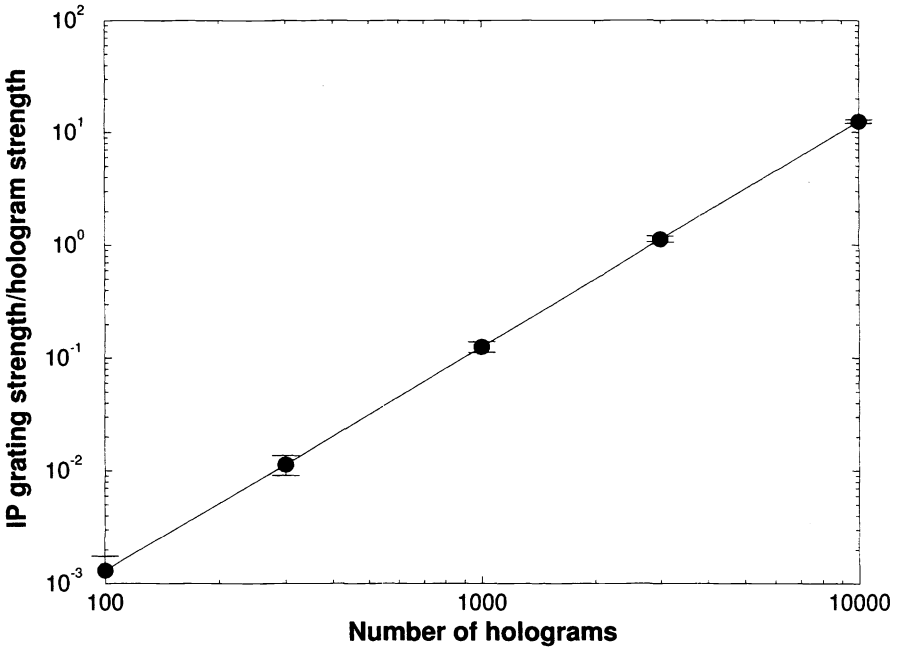

Figure 6. Ratio of the diffraction efficiencies of the inter–pixel grating $\vec{K}_{ij}$ and the information grating $\vec{K}_{ri}$ as a function of the number of holograms recorded with the same schedule.

of pixels (i, j) on a image consisting of 1,000×1,000 pixels. The outside angle between $\vec{K}_i$ and $\vec{K}_j$ was chosen at 1°, and $\vec{K}_{ij}$ was assumed to be parallel to the **c**–axis of the crystal. We simulated the recording of 100, 300, 1,000, 3,000, and 10,000 holograms using an exposure schedule also determined numerically. The result is plotted in Figure 6. It shows that, although the modulation depth of the inter–pixel grating is much smaller (by a factor of $\approx$ 1,000 in this case), its final strength is more than 10 times stronger than the information grating as the result of prolonged, repeated recording.

4. FORMATION OF INTER–PIXEL GRATING NOISE

The above discussion explains how an inter–pixel grating is formed during the recording of multiple holograms. It shows that an inter–pixel grating does grow and can be stronger than an information grating after a large number of holograms are recorded. However, since the inter–pixel grating noise is a secondary effect (the noise comes from the rediffraction), the crosstalk noise at a pixel from another one via the inter–pixel grating is orders of magnitudes less than the signal (inversely proportional to the diffraction efficiency of the inter–pixel grating). What finally makes the inter–pixel grating noise a significant noise source is that it arises from the collective behavior of a large number of pixels via a large number of noise gratings. In an image consisting of $N \times N$ pixels. a pixel writes inter–pixel gratings with all the other $(N^2 - 1)$ pixels during recording. Upon readout, it receives crosstalk noise from the other $(N^2 - 1)$ pixels via the "direct" Bragg–matched diffraction. In addition, crosstalk between pixels can take place via "indirect" diffraction, which is the result of Bragg degeneracy and weak Bragg selectivity. In the following discussion, we present a simple example of this collective effect.

For Fourier–transform–plane recording as shown in Figure 7(a), the crystal is placed at the focal plane of the Fourier–transform lens. The pixels on the SLM are converted into plane waves by this lens. The plane waves form a signal cone on the K–sphere. Normally, the size of the SLM is much smaller than the focal length of the FT lens. Therefore, by paraxial approximation, this cone on the surface of the K–sphere becomes a plane as shown in Figure 7(b). As a result, the inter–pixel gratings formed in between the plane waves all lie in this plane (with no z–components). When all the inter–pixel gratings are on the same plane, the crosstalk between pixels can only occur through Bragg–matched or Bragg–degenerate diffractions. In other words, two pixels only interfere with each other

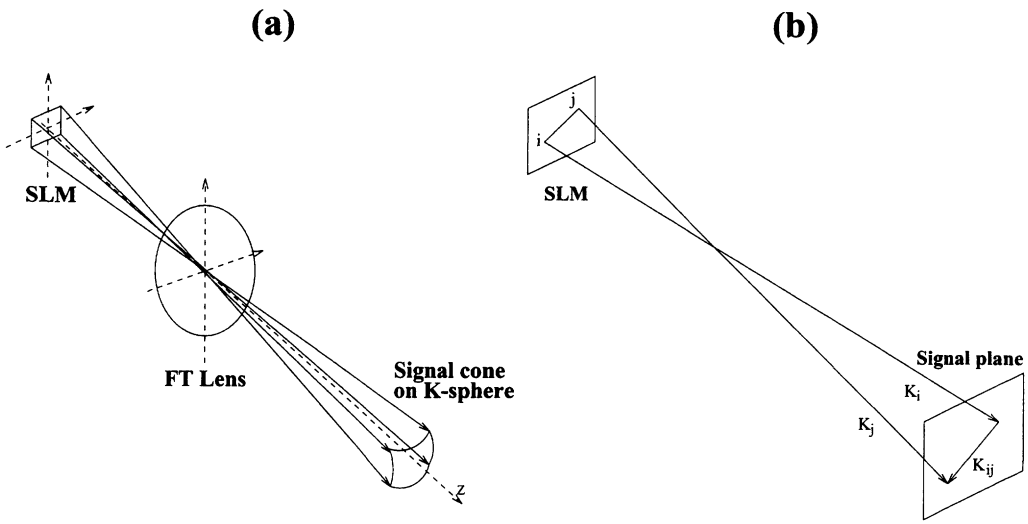

Figure 7. Signal cone (a) and signal plane (b) in Fourier–transform–plane recording.

via the grating they form directly and other degenerate gratings with the same grating vector (same orientation and magnitude). As shown in Figure 7(b), the signal plane formed by the tips of all the plane–wave components of the signal can be treated as the "image" of the SLM (from "pixel space" to "grating space"). The grating vector of one inter–pixel grating in the signal plane can be determined by the relative position of the two pixels on the SLM that write this grating. As a result, the analysis of the "connection" between the pixels can be carried out directly on the SLM plane.

Figure 8 shows the SLM plane where there are three "links" [§] between three pairs of pixels. The relative position of pixel j with respect to pixel i is the same as that of j' with respect to i':

$$d_x = d_{x'}\ ;\ \ d_y = d_{y'}. \tag{1}$$

Therefore, the links $\vec{K}_{ij}$ and $\vec{K}_{i'j'}$ are degenerate. As a result, crosstalk occurs between pixel i and j via the direct link $\vec{K}_{ij}$, as well as the indirect "link" $\vec{K}_{i'j'}$.

The total number of "links" from or to a pixel at (x, y) is the summation of all the "links" (direct and degenerate) between it and all the other pixels in the same image[¶]. It is written as

$$N_{total}(x,y) = \sum_{\substack{x'=0 \\ x' \neq x}}^{N-1} \sum_{\substack{y'=0 \\ y' \neq y}}^{N-1} (N - \frac{|x-x'|+1}{2})(N - |y-y'|), \tag{2}$$

where $N_{total}(x, y)$ provides the information about how well a pixel is "connected" to others, in which each "link" accounts for an increment in the crosstalk noise the pixel sees. Therefore, it shows how "noisy" it is at the pixel at (x, y). The equation also shows that the crosstalk noise is not uniform across the image. The worst case occurs at the center pixel. On an image of 1,000×1,000 pixels, there are over 1×10^{12} "links" to or from the center!

In practice, not all the "links" are degenerate. Instead, a large portion of the crosstalk takes place via Bragg–mismatched diffractions. In addition, the strength of the gratings varies as the result of different effective electro–optic and photovoltaic effect, as their grating vectors deviate from the c–axis[‖]. We conducted numerical simulations on the formation of the inter–pixel grating noise based on more rigorous theoretical treatment. The results suggest that it dominates the "inter–hologram" crosstalk as the leading noise source of a large–scale holographic stroage system.

[§] We prefer to use "links" instead of "gratings" because this is not the signal plane where the inter–pixel grating vectors lie. However, they represent the same concept in our analysis.

[¶] A pixel can be "connected" to another one via multiple "links".

[‖] e.g. the inter–pixel gratings are very weak if their grating vectors are at large angles to the c–axis.

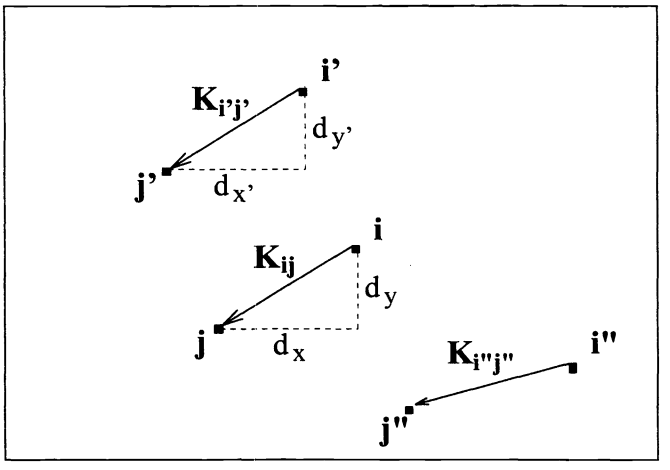

Figure 8. "Links" inducing crosstalk between a pair of pixels separated by horizontal and vertical distances d_x, d_y.

5. RANDOM–PHASE MODULATION IN THE SIGNAL

The effect of the inter–pixel grating noise is difficult to remove becasue it is a global, not a local noise source. On the other hand, the noise is not uniform across the entire image. Therefore, position–dependent threshold has to be applied to retrieve binary information with minimal errors, which complicates detection and data processing. In addition, since the amount of noise at a pixel depends strongly on the data structure of its neighborhood, effective elimination can not be achieved by "post–recording" compensation.[9,3]

Prolonged, repeated strengthening during multiple–hologram storage is a key factor in the formation of the inter–pixel grating noise. Therefore, if the phase difference between the plane waves corresponding to the pixels is randomly and continuously modulated at either zero or π during exposure, the final grating strength as a result of "positive" and "negative" recording shall be greatly reduced. In the meantime, a real information hologram is not affected except for the extra phase excursion added to each pixel which would not be sensed by the CCD because of intensity detection. In this section, we show the experiment results of using random–phase modulation to reduce the inter–pixel grating noise.

5.1. SUPPRESSION OF INTER–PIXEL GRATINGS WITH PHASE MODULATION

We repeated the previous experiments with a slight change in the signal arm (Figure 9). To randomly control the phase difference between the two plane–wave beams, a Liquid Crystal Phase Retarder (LCPR) (Meadowlark D1040) was used in the signal path. The fast and slow axes of the liquid crystal device were at 45° to the lab axes. An alternating signal was applied to the device to induce a change in the extraordinary refraction index. As a result, the phase difference between the two eigen–modes travelling through the device can be controlled electronically. A half–wave plate was placed in front of the LCPR to align the two linearly polarized plane–wave beams with the fast and slow axes of the LCPR. After the device, a phase difference of either 0 or π was imposed onto the two beams. A polarizer followed the LCPR to filter out unwanted polarization.

In the demonstration with random–phase modulation, we used a random–number generator to determine whether the phase difference between the two beams was to be set at 0 or π before recording a new hologram. At the end of recording, the same procedure was followed to yield the ratio of the strength of the inter–pixel grating and the holograms as a function of the number of holograms. The results from the experiments are summarized in Figure 10, together with the one from the previous experiments for comparison (Figure 10(a)).

Figure 10(b) shows that the strength of the inter–pixel grating can be greatly reduced by random–phase modulation. However, the reduction is not significant when the number of holograms is small. This could be attributed to the fact that the ON/OFF states of the two plane waves and their phase difference were controlled randomly and independently. If the number of holograms is small, there are no enough samples to average out the grating

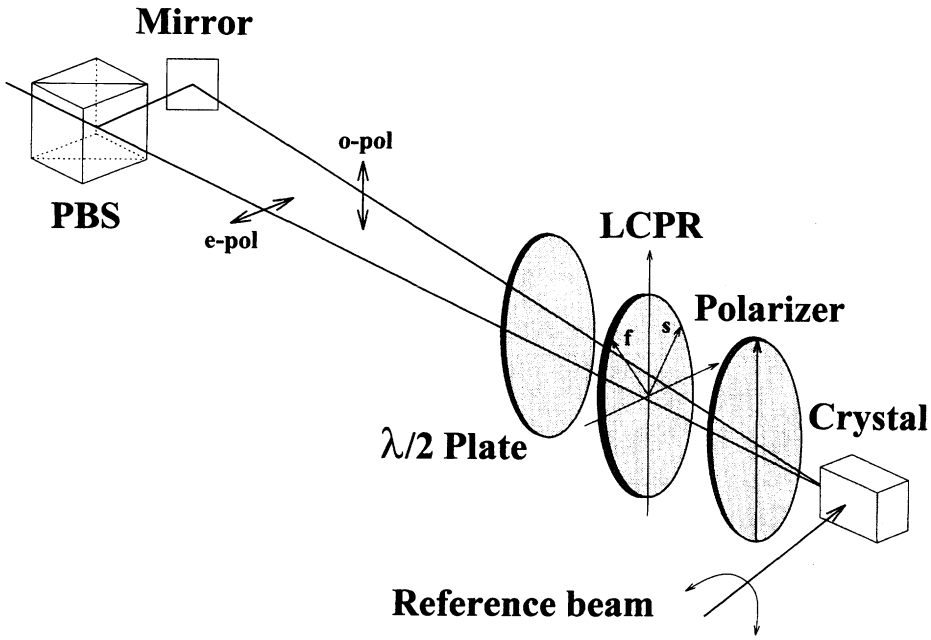

Figure 9. Experimental setup for the plane–wave signal experiment with random–phase modulation.

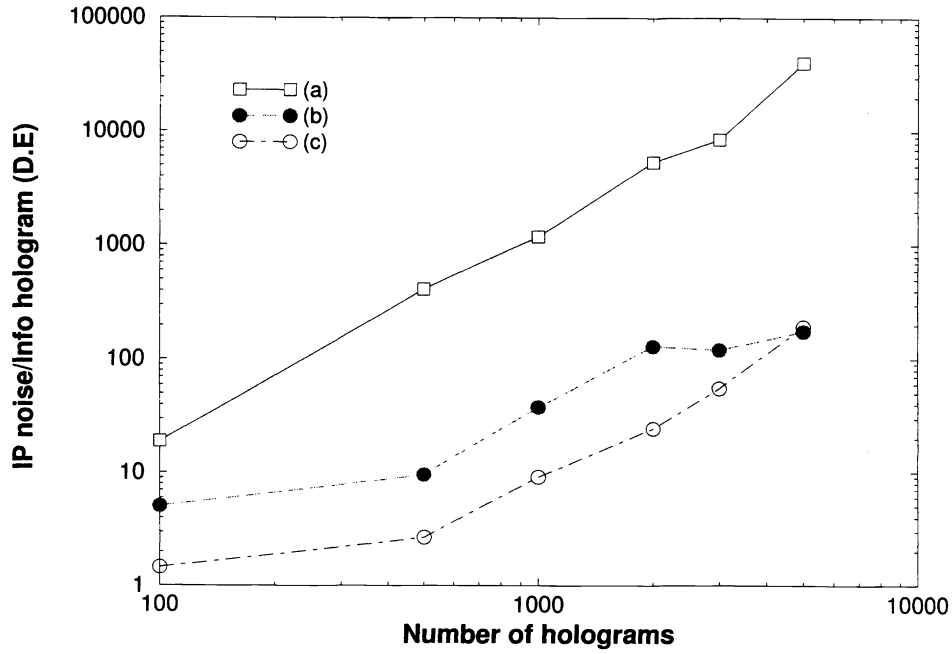

Figure 10. Ratio of the diffraction efficiencies of the inter–pixel grating and the hologram as a function of the number of holograms (a) without phase modulation; (b) random–phase modulation all the time; (c) π phase shift only when the two beams were ON at the same time.

buildup by "positive" and "negative" recordings. In order to observe the "ideal" effect of phase modulation, we chose a different way to control the phase difference in another set of experiments. Before the recording of a new 2–bit hologram, the ON/OFF states of the two bits (beams) were compared. If they were to be both ON, a new phase difference was set which was shifted by π with respect to the old one. This guaranteed that whenever the inter–pixel grating was to be strengthened, the exposing pattern underwent a π phase shift relatively, which "nullified" the previous buildup. The result from this set of experiments is also shown in Figure 8. As indicated by curve (c), the strength of the inter–pixel grating was further weakened. It is interesting to note that curve (b) and (c) seem to converge at a non-zero value. This means that even with random–phase modulation, the inter–pixel grating can not be completely eliminated. Intuitively, during repeated recording of a hologram at the same angle location with a "perfect" exposure schedule, the alternating "positive" and "negative" recording as used in our experiments would leave nothing recorded at all. However, in a holographic memory, the exposure schedule was determined by the dynamics of the buildup of the information holograms (in 90°–geometry recording in our case), while the buildup of an inter–pixel grating is different in terms of the time constant. As a result, the "perfect" exposure schedule for the information holograms is not perfect for the inter–pixel gratings. After the repeated strengthening and weakening by phase modulation, residual gratings remain, leading to the crosstalk noise.

5.2. IMPROVING SYSTEM ERROR PERFORMANCE BY PHASE MODULATION

In this section, we investigate the effect of the random–phase modulation on the error performance of a holographic memory system storing binary random–bit patterns. With random–bit patterns, there are enough samples in the reconstruction that allow us to use the Signal–to–Noise Ratio (SNR) to evaluate the system error performance statistically. In addition, the formation and influence of the inter–pixel grating noise as the result of the collective effect among many pixels can be revealed. Another advantage is the simplified experiment procedure—we can use the complex signal alone to illuminate the crystal to keep track of the evolution of the inter–pixel grating noise.

To generate the random–bit patterns, we used a graphics mode in BASICA which has 640× 200 pixels on VGA display. The SLM was an EPSON TVT6000 Liquid Crystal TV with 480× 440 pixels. Since the computer was not capable of generating the random–bit patterns in real time, we prepared a library of 100 patterns before recording. These 100 patterns were cycled many times for the storage of a large number of holograms. Therefore, the recording sequence was not truely random.

There are two ways to randomly phase–modulate the signal. Ths first one involves two Spatial Light Modulators: one operates in intensity–modulation mode and displays the information to be stored; the other lies in the image plane of the first one and phase–modulates the signal at the pixel level. The phase–modulated image is then focused at the crystal by a Fourier–transform lens. During exposure for the recording of a page of imformation, the phase–modulation SLM (PM SLM) displays a series of binary random–bit patterns continuously to make the phase difference between the pixels time–varying and random. The CCD detector would only detect the image displayed on the intensity–modulation SLM (IM SLM) to retrieve the stored information. However, this method had several drawbacks.

- The SLMs are very lossy because of their pixelation and small fill factor (usually, the light obtained in the filtered DC portion is only 10%). A large amount of light was wasted by stacking two SLMs together.
- For optimal random–phase modulation, the PM SLM needs to display the random–bit patterns very rapidly.
- It complicates the system hardware, including precision imaging optics, an additional SLM and control electronics, etc.

Alternatively, a single SLM can be used for both displaying and random–phase modulating the signal. This could be carried out with a phase–modulation SLM (PM SLM) which encodes the information as phase shift 0 or π at the pixels. All the pixels on the SLM are "ON" all the time since the information is embedded in the phase, not in the amplitude. As a result, all the inter–pixel gratings are recorded every time when a new hologram is added to the memory. However, since the possibilities of one pixel being either 1 or 0 (phase–shifted by 0 or π) are the same in a random–bit pattern, the possibility of two pixels being in the same state is 1/2. On the PM SLM, when two pixels are in the same state, the phase difference between them is zero. On the other hand, the phase difference is π when the two pixels are in different states. Therefore, although a pair of pixels continuously write the inter–pixel grating during hologram recording, during half of the exposures on average, the recording is

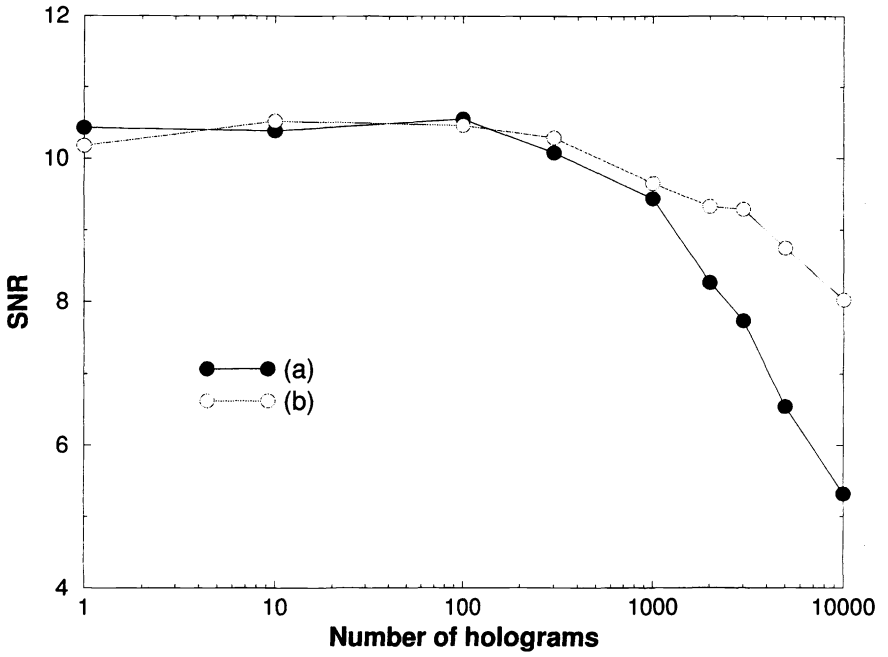

Figure 11. SNR as a function of the number of holograms: (a) without random–phase modulation; (b) with random–phase modulation.

"positive" (strengthening); while in the other half, the recording is "negative" (weakening). As a result, the strength of the inter–pixel grating could be greatly reduced by the random–phase modulation that arises from the random occurrence of the binary random–bit patterns to be stored in the memory. This method significantly simplifies the system hardware. Other advantages include the improved light efficiency (all the pixels on the PM SLM are ON all the time) and well distributed Fourier spectrum in Fourier–transform–plane recording. However, the use of PM SLM raises problems in the detection. Since the information is embedded in the phase, special techniques are required to translate the phase information into intensity information for data detection and retrieval. This can be done with an interferometer. But the interferometers are very sensitive to the environment such as air current and mechanical vibrations. Alternatively, edge–enhancement of the reconstructed holograms can be applied at the expense of weaker signal and lower capacities. A better approach might be the application of a specially designed phase plate similar to the phase–contrast microscope invented by Zernike sixty years ago. The basic idea is to introduce different phase excursions in different portions of the Fourier spectrum of the reconstruction which will translate the phase–modulated signal back to intensity modulation. This would not cost a great loss in the light intensity but might result in lower capacity.

We first simulated the recording without phase modulation. A single hologram, 10, 30, 100, 300, 1,000, 2,000, 3,000, 5,000, and 10,000 holograms were "recorded" by illuminating the crystal with a sequence of random–bit patterns according to an exposure schedule. At the end of every simulation, a random–bit pattern was displayed on the SLM. The transmitted signal was then sensed by a CCD camera (Photometric Imagepoint CCD) and sent to a computer for data analysis. By doing this, the signal was the direct transmission while the noise was its diffraction via the inter–pixel gratings. The SNR of the transmitted images is summarized in Figure 11(a). It drops from 10.3 from a single hologram down to 5.2 when 10,000 holograms were "stored," indicating significant influence of the inter–pixel grating noise as the total exposure increases.

In the experiment with random–phase modulation, we did not use any special techniques in signal detection. Instead, after simulating the storage of a certain number of holograms, the PM SLM was reconfigured back in intensity–modulation mode. The SLM displayed a random–bit pattern, and the transmission through the crystal was detected and processed. The SNR as a function of the number of holograms is also shown in Figure 9. As shown by curve (b) in Figure 11, the system error performance was improved significantly by random–phase modulation.

6. CONCLUSION

We have experimentally proved that the inter–pixel grating noise is a very important noise source in holographic memories using $LiNbO_3$. We have also demonstrated the use of random–phase modulation in the signal to reduce this noise. Future work is going to be directed at finding a practical phase–encoding and detection technique.

ACKNOWLEDGMENTS

We would like to thank Yunping Yang for his assistance. This work is supported by Rome Laboratory, USAF.

REFERENCES

1. L. Hyuk, X. Gu, and D. Psaltis, "Volume holographic interconnections with maximal capacity and minimal cross talk," *Journal of Applied Physics* **65**, pp. 2191–2194, March 1989.
2. M. P. Bernal, G. W. Burr, H. Coufal, and M. Quintanilla, "Optimizing the CCD fill factor to balance inter–pixel crosstalk and thermal noise in holographic data storage," in *OSA Annual Meeting, Paper ThB2*, (Long Beach, CA), 1997.
3. G. W. Burr, "Elimination of nonrandom noise in holographic data storage," in *OSA Annual Meeting, Paper ThB5*, (Long Beach, CA), 1997.
4. G. Burr, X. An, D. Psaltis, and F. Mok, "Large–scale rapid access holographic memory," in *1995 Optical Data Storage Meeting, SPIE Technical Digest Series*, vol. 2514, pp. 363–371, (San Diego, CA), 1995.
5. D. Psaltis, D. Brady, and K. Wagner, "Adaptive optical networks using photorefractive crystals," *Applied Optics* **27**(9), pp. 1752–1759, 1988.
6. N. V. Kukhtarev, V. B. Markov, S. G. Odulov, M. S. Soskin, and V. L. Vinetskii, "Holographic storage in electrooptic crystals. I. steady state," *Ferroelectrics* **22**, pp. 949–960, 1979.
7. C. Gu, J. Hong, H. Y. Li, D. Psaltis, and P. Yeh, "Dynamics of grating formation in photovoltaic media," *Journal of Applied Physics* **69**(3), pp. 1167–1172, 1991.
8. G. W. Burr and D. Psaltis, "Effect of the oxidation–state of $LiNbO_3$:Fe on the diffraction efficiency of multiple holograms," *Optics Letters* **21**(12), pp. 893–895, 1996.
9. X. An and D. Psaltis, "Experimental characterization of an angle–multiplexed holographic memory," *Optics Letters* **20**(18), pp. 1913–1915, 1995.